Environment and Climate Protection (2024)
Clausius Scientific Press, Canada

DOI: 10.23977/envcp.2024.030102
ISSN 2523-6504 Vol. 3 Num. 1

Study on Soil Moisture Dynamics and Fitting in Mu Us Sandy Land

Xianghan Liang

Management Committee of Beijing Olympic Park Central Area, Beijing, 100101, China

Keywords: Soil water content; Precision; Dynamics; Mu Us sandy land

Abstract: In order to deeply analyze the spatiotemporal dynamics of soil moisture in Artemisia Ordosica sample plots with different fixed degrees (fixed, semi fixed, and shifting sand land) in Mu Us sand land, this study conducted long terms and continuous monitoring of soil moisture in three types of sample plots by using the AR-5 automatic soil moisture monitoring system, And used AV-3665R rainfall sensor to monitor rainfall The results showed that: (1) In the study area, the seasonal variation of soil moisture was fundamentally synchronized with precision, the change trend of soil water content is significantly related to precision Under the joint influence of precision, plant root distribution and evaporation, the spatial dynamics of soil water in three sample plots with different degrees of fixation are significantly different In each time period, the soil water content of fixed sand land is less than that of semi fixed sand land and shifting sand land. (2) Every year, the change of soil water content is generally divided into three periods From November to February, the soil moisture content increased steadily; From March to July, the soil water content first increased significantly, then decreased slowly; From August to October, the soil water content increased significantly. (3) The vertical distribution layer of soil water content in different fixed types of sandy land can be divided into four layers, named the soil water sharp change layer (0-10cm), the soil water sensitive layer (10-40cm), the soil water active layer (40-120cm), and the soil water stable layer (120-200cm). (4) The fractional soil water movement model is used to simulate the soil water dynamics, and the parameters are modified after the preliminary validation of the model The results show that the model parameters after the parameter correction meet the set value range, and the goodness of fit meets the statistical requirements, and the modified model can better reflect the soil water movement in different periods. (Figure 6, Table 2, Reference 13)

The northwest region of China has low precipitation, strong evapotranspiration, and low soil moisture, resulting in various arid and semi-arid landforms and landscapes, forming a desert ecosystem [1-3]. The formation and succession process of desert ecosystems are closely related to water, and water is one of the most active components in the system [4-6]. Precipitation, artificial irrigation, and condensed water all need to be converted into soil water through infiltration before they can be absorbed and utilized by plants. Soil water refers to the water content in the soil layer from the surface of the soil to the groundwater level above. It is an important component of water resources in desert ecosystems and serves as a bridge connecting precipitation, surface water, atmospheric water, and groundwater. In arid and semi-arid areas, soil moisture severely restricts plant growth and

development, and land degradation is directly related to the decrease in soil moisture content. Therefore, research on soil moisture is of great significance for local vegetation restoration and reconstruction.

The Mu Us Sandy Land is located in the agricultural pastoral transitional zone of China and is an important ecological barrier in northern China. *Artemisia ordosica* is one of the most important constructive and dominant species in the local area. 29.9% of the sand area is the Artemisia annua community, which is the largest area of local plant communities. Artemisia annua has advantages such as drought resistance, sand burial resistance, and wind erosion resistance, and plays a key role in the stability of the local ecosystem. Existing studies have shown that the natural succession process of Artemisia annua communities is characterized by mobile sandy land (pioneer species stage) - semi fixed sandy land (sparse stage) - fixed sandy land (built-up stage) - old fixed sandy land (degradation stage) - mobile sandy land. Scholars have conducted relevant research on the soil moisture content of Artemisia annua communities at different stages of succession in the Mu Us sandy land, and the impact of soil moisture on the succession of Artemisia annua communities, and have made certain research progress [7-11]. However, previous monitoring of soil moisture content in the Mu Us sandy land was mostly timed and fixed-point sampling, lacking continuous monitoring data, which could not fully meet the research requirements of researchers on the spatiotemporal dynamics of soil moisture in the Mu Us sandy land [12-13]. This study conducted long-term continuous monitoring of soil moisture in the 0-200cm soil of Artemisia annua communities on fixed, semi fixed, and mobile sandy land, and analyzed the soil moisture dynamics of Artemisia annua communities at different succession stages during the growing season. The aim was to explore the role of soil water in the ecosystem, in order to provide theoretical basis for the scientific allocation of vegetation density in Artemisia annua communities.

1. Experiment site

Table 1: Basic Information of the Sample Land in the Study Area

stage Stage	**type Type**	**Vegetation and Surface features Characters in land surface And cultivation**	**vegetation coverage (%) Vegetation coverage (%)**
Pioneers Seed stage	flow sand	The main plants include scattered species such as sand rice, sand bamboo (*Psammochloa villosa*), Artemisia annua, and Artemisia annua, which have no crust cover and are prone to wind erosion due to loose soil	5-20
sparse stage	Semi fixed sand	The main plants include Artemisia annua, Artemisia annua, and *Leymus secalinus*, with a surface crust thickness of 0.1-0.4cm and a coverage of about 30%	20-30
Built stage	fixed sand	The main plants include Artemisia annua, *Suaeda glauca*, *Setaria viridis*, etc., with a surface crust thickness of 0.5-1.5cm and a coverage of about 80%	30-50

The research area is located in Wushen Banner, Ordos City, Inner Mongolia Autonomous Region, which is the central area of Mu Us Sandy Land. The sand area of Mu Us Sandy Land is 41900 square kilometers, with coordinates of 37 ° 26.5 ′ -39 ° 21.5 ′ N and 107 ° 20.4 ′ -111 ° 30.3 ′ E, with an overall elevation between 1150 meters and 1350 meters. The research area is located west of the 400mm equal precipitation line in China and belongs to a temperate continental climate. The annual average precipitation fluctuates between 270-350mm, and the distribution is extremely uneven

throughout the year. The highest precipitation occurs from July to September each year, accounting for more than 75% of the annual precipitation. The interannual distribution of precipitation is also extremely uneven, with the highest annual precipitation within 50 years being 548mm and the lowest being only 185mm, with a difference of nearly three times. The annual average temperature is 6.5 ℃, the average temperature in January is -10.3 ℃, and the extreme minimum temperature is -31.4 ℃; The average temperature in July was 22.5 ℃, with an extreme maximum temperature of 36.8 ℃. The study area has frequent wind and sand activities, and the surface soil is loose. Therefore, sandy vegetation and grassland vegetation dominated by natural vegetation. Perennial herbs and shrubs such as Artemisia *sphaerocephala krasch*, *Salix cheilophila*, and *Artemisia sphaerocephala krasch* are constructive and dominant species in the ecosystem, followed by first and second year herbs such as *Agriophyllum squarrosum. There are* not many species of tall shrubs and trees. Artemisia annua is the most important community building species in the region and is also the preferred species for planting and aerial seeding [12]. The vegetation characteristics of different fixed types of sandy land in the study area are shown in Table 1.

2. Methods

This study adopted long-term continuous monitoring and focused on the inter hilly areas of Artemisia annua communities in fixed, semi fixed, and mobile sandy lands with slopes less than 5 degrees. Three repeated experiments were conducted on each sample plot. The average soil bulk density of the 0-200cm soil layer in the region is 1.71g/cm3, and the proportion of coarse sand (soil particle size 0.5-1mm) is 0.03%; The sand content in the middle (0.1-0.5mm) is 87.36%; Fine sand (<0.1mm) accounts for 12.61%. A 200cm deep soil profile was excavated from the bare sand surface without crust covering between two Artemisia annua plants to install an AR-5 soil moisture automatic monitoring system, which includes 5 EC-5 detectors and an AR-5 data collector. EC-5 is a soil moisture detector developed by the American company Decagon. Its working principle is based on the correlation between soil moisture content and soil dielectric constant. Through the electronic oscillator on the instrument's circuit board, it continuously emits a 75MHz square electromagnetic wave to measure the dielectric constant of the soil near 1cm away from the detector. The instrument's internal data analysis system converts the dielectric constant into soil moisture content and monitors the data every 30 minutes. Due to the low factory precision of EC-5, it cannot meet the research requirements of arid and semi-arid areas. In 2013, Wu et al. considered various factors such as soil temperature, soil texture, and soil bulk density under natural conditions, and used the drying method to calibrate the EC-5 sensor [13]. The calibration equation is:

$$C=0.1506-0.001506mv+3.218\ (mv)^{2}$$

Among them, C represents the corrected soil moisture content (m3 ·m-3), and mv represents the output reading of the EC-5 sensor ($^{m3\ \cdot m-3}$). The soil moisture data used in this study were all derived from calibration equations. The function of the AR-5 data collector is to provide data storage and power supply for EC-5. The installation depth of each set of EC-5 sensors is 10cm, 20cm, 40cm, 60cm, 80cm, 100cm, 120cm, 160cm, and 200cm respectively, with a total of nine layers. The basic level of groundwater in the research area is generally below 6 meters, so the soil moisture content of 0-200cm is not affected by groundwater. Starting from October 2013, instruments were installed and rain gauges were set up to measure precipitation. The period from October 2013 to February 2014 was used as the soil disturbance recovery period, and the data recorded from March 2014 was used as effective data to analyze the soil moisture dynamics during the growing season of that year. The data was processed using SPSS 16.0 and Excel 2013, with mean ±SE representing the mean and one-way analysis of variance (LSD) for significance difference (a=0.05).

Using a fractional order soil moisture movement model to predict soil moisture. This model was

initially used for dynamics and gradually applied to other studies. When using numerical methods to represent soil water storage in a fully discrete form, there exists a recursive equation between soil water storage at different time periods as follows:

$$W=W_0+\frac{1}{W_0}\left(\sum_{i=0}^{n} a_{j,r+1}F\left(d_j,x\right)+a_{r+1}F\left(t_{r+1},x\right)\right) \quad (1)$$

Among them, a, r, j, b, c, d, and f are the fitting coefficients, W is the soil water storage (dependent variable), W_0 is the soil water storage at the previous moment, X is the environmental factor (independent variable), and the operation represented by F is:

$$F\ (d,\ x)=\frac{\partial}{\partial x}\left(D_r\ (x)\ \frac{\partial y}{\partial x}\right) \quad (2)$$

The basic algorithm of D_r is:

$$D_r=\frac{r_s b_d}{n(c_s-f_d)}\left(\frac{r_s-r_0}{r-r_0}\right)\frac{n-1}{n} \quad (3)$$

Assumption:

$$R=\frac{r_s-r_d}{r_s-r_0} \quad (4)$$

So, equations 1 can be written as:

$$-\frac{\partial}{\partial x}K_r\frac{\partial h}{\partial x}=-\frac{\partial}{\partial x}\left(-\frac{K_s h_d}{n}\frac{\partial y}{\partial x}\frac{n-1}{n}\right) \quad (5)$$

And:

$$\frac{\partial y}{\partial x}=\frac{1}{\gamma\ (1-r)}\int_0^r\frac{\frac{\partial y}{\partial a}}{(r-a)^b}da \quad (6)$$

The necessary and sufficient condition for the existence of an extremum in this equation is that the extremum solution satisfies the Euler equation, and it can be assumed that:

$$F\ (a,\ h,\ d)=\frac{h^{m-n}}{h+cosr} \quad (7)$$

According to equations 6:

$$(1^{-chn}-mcosr)^{-1/1=}cosr\frac{da}{dh} \quad (8)$$

By applying the integral mean value theorem, it can be obtained that:

$$\frac{1}{n-m}=\int\frac{1-cycosr}{y}dy=\int coscr\ dz \quad (9)$$

Among them, y satisfies the following conditions:

$$y=h^{n-m} \quad (10)$$

Therefore, it can be concluded that:

$$ccosr=\left(\frac{1}{h}\right)^{m-n}=1-\left(e^{\frac{m-n}{2ah}(z+c)cosr}-1\right) \quad (11)$$

From 5 and 11, it can be concluded that:

$$\left(\frac{r_s-r_0}{r-r_0}\right)^{\frac{m-n}{n}}=\frac{1}{ccosr}\left(1-e^{\frac{m-n}{2ah}(z+c)cosr}\right) \quad (12)$$

The functional extremum solution is:

$$r=r_0+r_s \frac{e^{\frac{nzcosa}{2ah_d}}\left(1-\frac{e^{e^{\frac{nzcos2a}{2ah_d}}}}{e^{e^{\frac{nzcosa}{2ah_d}}}}\right)a^{\frac{n}{m-n}}}{} \approx r_0+r_s e^{\frac{nzcosa}{2ah_d}}\left(1-\frac{ab}{d}\right)e^{\frac{n}{m-n}} \tag{13}$$

When the difference between r and r_0 is large, the functional extremum solution is corrected as follows:

$$r=r_0+r_s\, r_s e^{\frac{nzcosa}{2ah_d}}\left(1-\frac{ab}{d}\right)e^{\frac{n}{m-1-n}} \tag{14}$$

The difference between the m-th and n-th measurement results and the derivative of the time difference t are approximated using the L approximation criterion in the Ca derivative method. The central difference quotient can be expressed as:

$$\frac{t^{-a}}{[r(1-a)}+a^b-\sum_{k=1}^{n-1}a_{n-k-1}-a_{n-k-m}-a_{n-1}]\frac{d}{dx}\left(\frac{dc}{dx}\right)= \tag{15}$$

$$\frac{D_{j+1}^n\left(a_{m-1}^n+a_j^n\right)+D_{j-1}^n\left(a_{m-1}^n+a_{j-1}^n\right)+D_{j+1}^m\left(\left(a_{m-1}^n+a_j^n\right)+D_{j-1}^m\left(\left(a_{m-1}^n+a_j^n\right)\right.\right.}{(\triangle x)^2}$$

From this, it can be concluded that the fully discrete format of the equation for the variation of soil water storage over time can be expressed as:

$$W= r_0+\sum_{k=1}^{n-1}(a_{n-k-1}-a_{n-k-m}-a_{n-1})r_s e^{\frac{nzcosa}{2ah_d}}+ \tag{16}$$

$$\frac{D_{j+1}^n\left(a_{m-1}^n+a_j^n\right)+D_{j-1}^n\left(a_{m-1}^n+a_{j-1}^n\right)+D_{j+1}^m\left(\left(a_{m-1}^n+a_j^n\right)+D_{j-1}^m\left(\left(a_{m-1}^n+a_j^n\right)\right.\right.}{(\triangle x)^2}$$

The boundary conditions are:

$$r_n=r_s \tag{17}$$

$$r_{m-1}^n=r_0 \tag{18}$$

The initial conditions are:

$$r_0^i=r_0 \tag{19}$$

The numerical solution of equations 5 is:

$$W=\sum_i(r_{x_i}-r_0)\ \triangle x \tag{20}$$

$$i=\frac{K_a h_d}{n(r_s-r_0)}\frac{dr}{dx}=\frac{K_a h_d}{n(r_s-r_0)}\frac{\sum_i(r_{x_i}-r_0)}{\triangle x}$$

The basic expression for the fitting equation of soil water storage capacity can be obtained as follows:

$$W=\frac{dK(r^m)}{dr}\frac{da}{dz}+D r_n^m-\left(\frac{hdK(r^m)}{2dr}\right)\frac{d^2c}{dc^2}-\frac{hD(r^m)d^3c}{2db^3}+\left(\frac{dKr^m}{dr}-\frac{dK^2r^m}{2hdr^2}\right)\left(\sum_{i=1}^n\frac{dc_i r_i}{dz}\right)-$$

(21)

$$\frac{dr_i}{2hdb^3}\frac{3h}{2}\frac{dKr^m}{dr}\left(\sum_{i=1}^{n}\frac{dc_ir_i}{db}\sum_{i=1}^{n}\frac{dc_ir_i}{dz}\right)\frac{d^2c_i}{dc^2}-()\frac{da_i}{df_i}$$

By substituting equations 20 and 21 and eliminating excess parameters, we can obtain:

$$W=\frac{dr_i}{2hdb^3}\left(\frac{d^2cx_2hdK(r^mx_1)}{dc^2\quad 2dr}\right)-\left(\sum_{i=1}^{n}\frac{dc_ir_i}{dbx_4}\right)\frac{da_{ix_3}}{df_i} \quad (22)$$

3. Result analysis

3.1 Precipitation characteristics in the study area

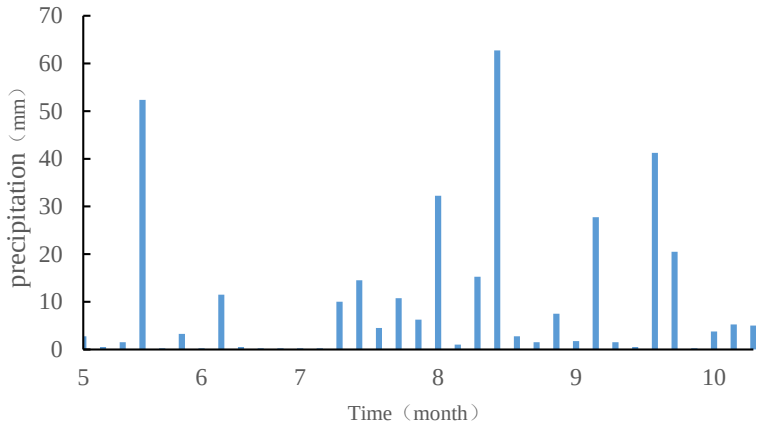

Figure 1: Rainfall situation during the growing season

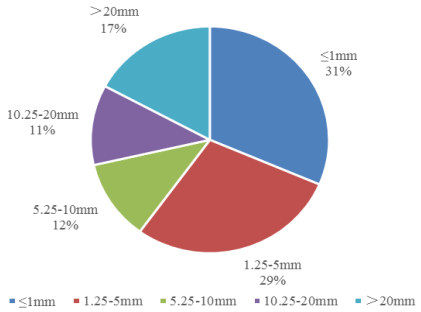

Figure 2: Distribution of precipitation frequency during the growing season

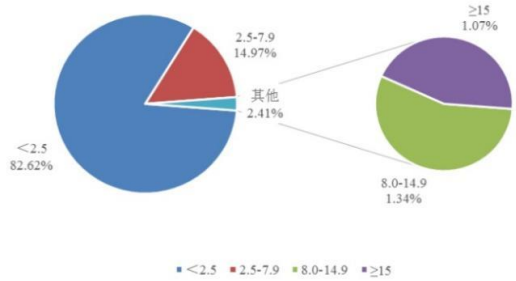

Figure 3: Distribution of Rainfall Intensity (mm/h)

There were a total of 41 rainfall events in the research area in 2013, with a total precipitation of 342.25mm. Among them, the growing season occurred 35 times, with a precipitation of 332.75mm, accounting for 97.2% of the annual precipitation. Most of the precipitation in the research area is mainly from light to moderate, with 28 occurrences of precipitation less than 10mm. The frequency of precipitation accounts for 67% of the total annual precipitation, but the precipitation only accounts for 18.19% of the annual precipitation; There were 10 instances of precipitation exceeding 10mm, with a precipitation of 266.35mm, accounting for 80.05% of the precipitation during the growing season; There were 5 times when the precipitation exceeded 20mm, with a precipitation of 173.15mm, accounting for 52.2% of the growth season precipitation. During the growth season, precipitation is most concentrated from July to September, accounting for 79.6% of the growth season (Figure 1, Figure 2). The distribution of rainfall intensity in 41 rainfall events is shown in Figure 3. The frequency of rainfall intensity less than 2.5 mm/h exceeds 80%, and only about 1% of rainfall intensity exceeds 15 mm/h. This indicates that precipitation in the study area is basically absorbed by the soil or lost through evapotranspiration, and generally does not form surface runoff.

3.2 Seasonal dynamics of soil moisture

The seasonal variation of soil moisture content in the study area is basically synchronous with precipitation and the trend of variation is mostly linear (Table 2). Precipitation has a significant impact on soil moisture content, which is negatively correlated with soil depth. The changes in soil moisture content in the 10-120cm layer each year are generally divided into three periods. From November to February, the precipitation is sparse, the soil has not yet thawed, and the evapotranspiration of plants is not strong during the non growing season. Therefore, the soil moisture content steadily increases, maintaining between 4% -7% From March to July, as the temperature rises, the soil thaws, resulting in a significant increase in soil moisture content during this period; Then the growing season gradually arrives, and the physiological activities of plants are significantly enhanced, with a sharp increase in transpiration. However, at this time, the precipitation is generally less, so the soil moisture content begins to slowly decrease, with a minimum value of 3% -5% From August to October, due to the arrival of the rainy season, the overall soil moisture content significantly increases.

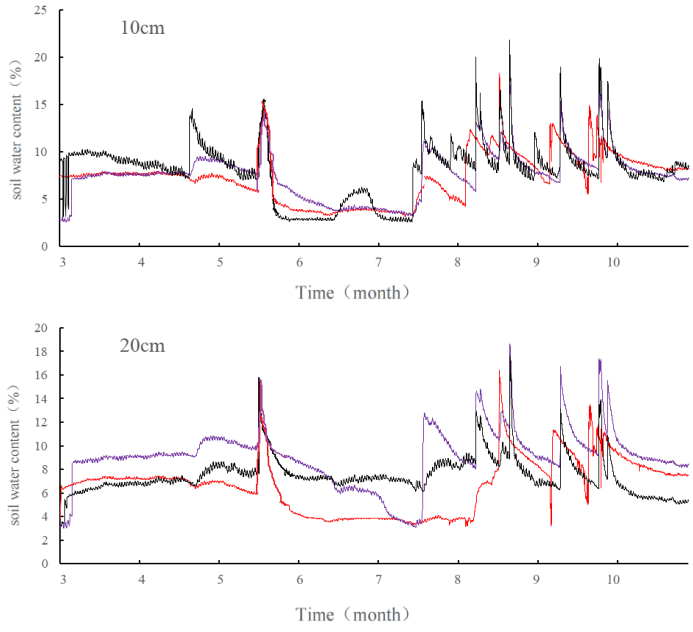

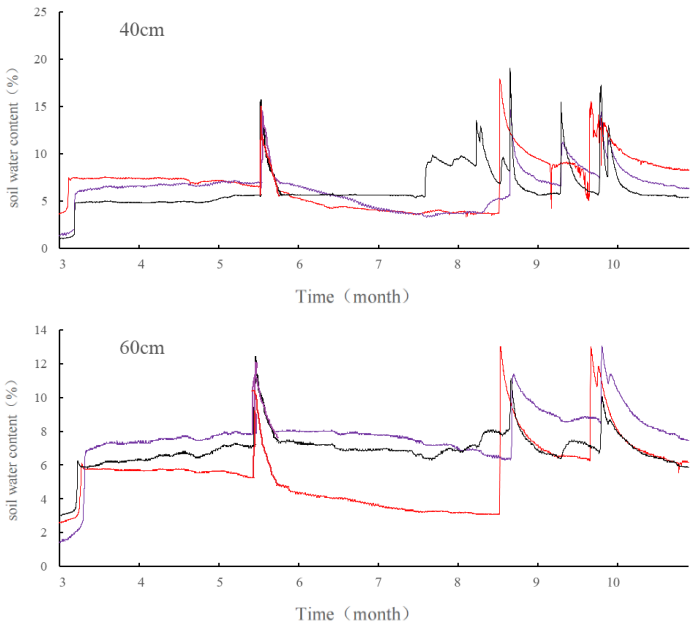

Figure 4: Seasonal dynamics of soil moisture

With the increase of rainfall frequency and rainfall in August, after each rainfall exceeding 10mm, the soil moisture content of the three types of plots will show a peak. The analysis of Figure 4 and the collected data shows that the peak time of soil moisture content corresponds one-to-one with the precipitation time, indicating a significant positive correlation between soil moisture content and precipitation. Starting from August, the soil moisture content in the 10cm, 40cm, 60cm, 80cm, 100cm, and 120cm layers of the three types of plots showed 8, 4, 3, 2, 2, and 1 peak, respectively. In the 20cm layer, there were 6 occurrences of mobile sand dunes, and 5 peaks were observed in both fixed sand dunes and semi fixed sand dunes. After the rainfall event on August 20th, the soil moisture content of three different fixed degrees of sandy land showed annual maximum values (Table 3). August and September are the periods with the richest precipitation of the year. Starting from October, precipitation gradually decreases, and the soil moisture content of different soil layers in various sample plots gradually decreases, with most of the downward trends showing a linear relationship. Starting from the end of October, as the temperature gradually decreases, the surface soil begins to freeze, and the soil moisture content of each soil layer tends to stabilize.

3.4 Model prediction

Model 2-22 and MATLAB software were used to predict soil moisture during the study period, and the fitting results are shown in Figure 6. The fitting effect of the model was tested by the measured values. Table 2 shows the fitting model parameters, determination coefficients, and fitting effect tests for different soil layers. The main purpose of establishing a fitting model is to simulate and predict changes in soil water storage throughout the entire growth season using environmental factors. From the table, it can be seen that the changes in soil water storage are mainly related to the total precipitation during the growing season, root biomass, and soil physical properties.

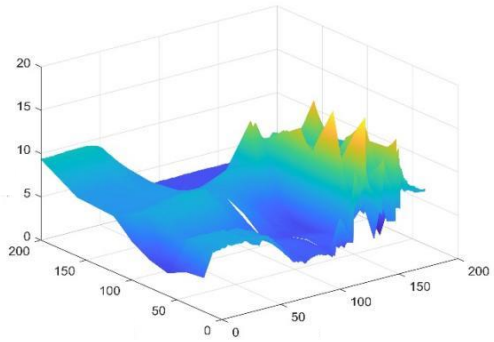

Fixed sandy land

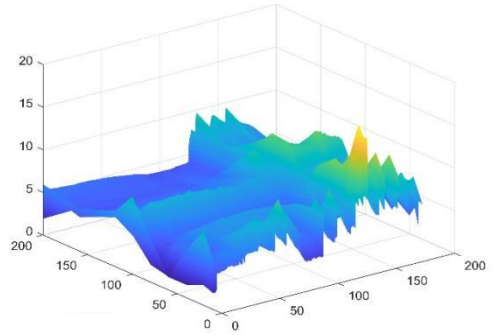

semi-fixed sandy land

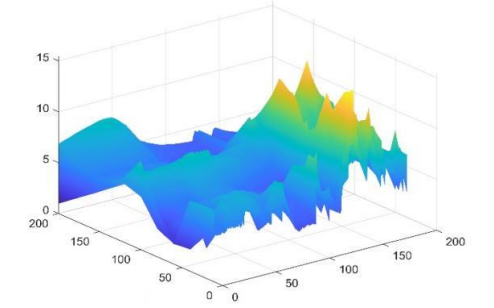

Flowing Sandland

Figure 5: Dynamic Fitting Diagram of Soil Moisture

4. Conclusion

(1) Within the research area, the seasonal variation of soil moisture content is basically synchronized with precipitation, and the trend of soil moisture content change is significantly correlated with precipitation. Under the joint influence of precipitation, plant root distribution, and evapotranspiration, there are significant differences in the spatiotemporal dynamics of soil moisture among the three types of plots with different degrees of fixation. During each time period, the soil moisture content of fixed sandy land is lower than that of semi fixed sandy land and mobile sandy land in each soil layer.

(2) Every year, the changes in soil moisture content are generally divided into three periods. From November to February, the soil moisture content remained stable with an increase; From March to July, the soil moisture content first significantly increased and then slowly decreased; From August to October, the overall soil moisture content significantly increased.

(3) The vertical distribution layer of soil moisture content in different fixed types of sandy land can be divided into four layers, namely: soil moisture dramatic layer (0-10cm), soil moisture sensitive layer (10-40cm), soil moisture active layer (40-120cm), and soil moisture stable layer (120-200cm). The variation of soil moisture content with soil depth is basically linear.

(4) The fractional order soil moisture movement model was applied to simulate the dynamics of soil moisture. After preliminary validation of the model, parameter corrections were made. The results showed that the model parameters after parameter corrections met the set value range, and the goodness of fit met statistical requirements. The revised model can better reflect the soil moisture movement situation in different periods.

References

[1] Feng Q. Advance in Sandy—land Moisture Research [J]. Journal of Desert Research, 1993, 13(2):9-13.

[2] Xiao D. Comments on the progress and direction in soil water research [J]. Ecology & Environmental Sciences, 2009, 18(3):1182-1188.

[3] AN Hui, AN Yu. Soil moisture dynamics and water balance of Salix psammophila shrubs in south edge of Mu Us Sandy Land. Chinese Journal of Applied Ecology [J].Sep. 2011, 22(9): 2247-2252.

[4] Cui Liqiang, Wu Bo, et al. The characteristics of soil water in different vegetation coverage on the southeastern margin Mu us sandy land. Journal of Arid Land Resources and Environment [J]. 2010, 24(2):177-182.

[5] Dong D G, Bo W U, Jun C L, et al. Present Situation, Cause and Control Way of Desertification in China [J]. Journal of Desert Research, 1999.

[6] Chao-Feng F U, Zhao J B. Distribution of Soil Moisture Content in Different Types of Sand Dunes in the Southeastern Marginal Zone of the Mu Us Sandy Land [J]. Arid Zone Research, 2011, 28(3):377-383.

[7] Guo, K., Dong, X. J., & Liu, Z. M. (2000). Characteristics of soil moisture content on sand dunes in Mu us sandy grassland: why Artemisia Ordosica declines on old fixed sand dunes. Acta Phytoecologica Sinica, 2000, 24: 275-279.

[8] Guo K. Cyclic succession of Artemisia ordosica Krasch community in the Mu Us sandy grassland [J]. Acta Phytoecologica Sinica, 24(2): 243—247, 2000.

[9] Zhi-Bin H E, Zhao W Z. Variability of Soil Moisture of Shifting Sandy Land and Its Dependence on Precipitation in Semi-arid Region [J]. Journal of Desert Research, 2002, 22(4):359-362.

[10] Bao H, Hou L, Shen J, et al. Research on soil water dynamics of farmland in Mu Us Sand Land [J]. Chinese Journal of Eco-Agriculture, 2014.

[11] Angusa J F, Gault R R.Soil water extraction by dryland crops, annual pastures, and Lucerne in South-eastern Australia. Australian Journal of Soil Research [J].2001, 52:183-192.

[12] Brown K W, Evans G B.Increased soil water retention by mixing horizons of shallow sandy soil.Soil Science [J].1985,139:118-121.

[13] Wu B, Han H Y, He J, et al. Field-specific calibration and evaluation of ECH2O EC-5 sensor for Sandy soils. Soil Science Society of America Journal, 2014, 78:70-78.